Accuracy of Coulomb Stripping for Measuring Single-Particle Reduced Widths in Nuclei*

FAISON P. GIBSON†
Oak Ridge National Laboratory, Oak Ridge, Tennessee

AND

ARTHUR K. KERMAN
Massachusetts Institute of Technology, Cambridge, Massachusetts

(Received 29 September 1965)

A finite-range *n-p* potential and the effect of deuteron stretch have been introduced into a distorted-wave Born-approximation (DWBA) analysis of the *d-p* stripping process for the case in which both deuteron and proton have energies below the Coulomb barrier. This energy region was chosen because it permits an estimate of the experimental reduced width which does not depend significantly on assumptions regarding the target interior. The stretch of the detueron wave function is calculated with the adiabatic approximation under the electric dipole perturbation of the target. The proton and neutron wave functions are Taylor-expanded about the center-of-mass coordinate of the deuteron as a series in the relative coordinate of the deuteron. The stripping matrix element is then expressed to second order in this parameter as a sum of five terms which are introduced into a modified version of the Gibbs-Tobocman DWBA stripping program. A series of calculations was made for the case of a Bi target in order to compare these second-order terms with the first-order term, which is just the usual zero-range approximation. The shape of the proton angular distribution was only modestly affected. The change in peak magnitude varied up to about 16% in the Coulomb-stripping region, with corresponding inverse effect on the experimental reduced widths which would be inferred therefrom. The effect of the nuclear potentials producing proton and deuteron elastic scattering is significant, but it is mostly contained in the region of the integrations and therefore depends mainly on the elastic-scattering phase shifts. We conclude that the particle reduced widths can be "measured" by Coulomb stripping to better than 10% as far as theoretical uncertainties are concerned.

INTRODUCTION

IN recent years there have been a number of differential cross-section calculations[1–4] for (d,p) stripping reactions by use of DWBA methods. With rare exceptions[5,6] these methods include an assumption of zero range for the neutron-proton potential and disregard the possibility of deuteron stretching during the stripping process. The present work[7] is an attempt to remove these deficiencies for the particular case of Coulomb stripping, i.e., for those situations in which the deuteron and proton energies are below the Coulomb barrier. This energy region permits certain convenient approximations and allows one to obtain fairly accurate estimates of experimental reduced widths which do not rely strongly upon any assumptions regarding wave functions and potentials in and close to the target. This comes about from the circumstance that the major contribution to the integral of the stripping matrix element comes from the region near the classical turning points while only a small contribution comes from the region within the target nucleus.

The Gibbs-Tobocman zero-range DWBA program has been modified to incorporate finite-range and polarization effects and a series of calculations made for the differential cross sections on a ^{209}Bi target for a variety of incident energies, Q values, and l values of the captured neutron. These cross sections have been compared with the zero-range results. We note that the unmodified program has been rather successfully used by Erskine *et al.*[8] to fit the shape of experimental angular distributions in this region.

APPROACH

The DWBA stripping matrix element employed is

$$T=\langle F_p^{(-)}(\mathbf{r}_p)u(\mathbf{r}_n,\xi_n)\,|\,V_{np}(r)\,|\,\psi_d^{(+)}(\mathbf{r}_p,\mathbf{r}_n)v(\xi)\rangle \quad (1)$$

$$=\langle F_p^{(-)}(\mathbf{r}_p)G_n(\mathbf{r}_n)\,|\,V_{np}(r)\,|\,\psi_d^{(+)}(\mathbf{r}_p,\mathbf{r}_n)\rangle \quad (2)$$

$$=\langle F_p^{(-)}(\mathbf{R}+\tfrac{1}{2}\mathbf{r})G_n(\mathbf{R}-\tfrac{1}{2}\mathbf{r})\,|\,V_{np}(\mathbf{r})\,|\,\psi_d^{(+)}(\mathbf{R},r)\rangle. \quad (3)$$

In these expressions $\mathbf{r}_p$ is the radius vector from target to proton, $\mathbf{r}_n$ is the radius vector from target to neutron, ξ is the collection of coordinates for the target nucleons, $\mathbf{r}=(\mathbf{r}_p-\mathbf{r}_n)$, $\mathbf{R}=\frac{1}{2}(\mathbf{r}_p+\mathbf{r}_n)$, $F_p^{(-)}$ is the scattering func-

* Research sponsored by the U. S. Atomic Energy Commission under contract with the Union Carbide Corporation and under AEC Contract AT(30-1)-2098.

† U. S. Atomic Energy Commission Postdoctoral Fellow under appointment from the Oak Ridge Institute of Nuclear Studies. Now at Stanford Research Institute, Huntsville, Alabama.

[1] W. Tobocman, Phys. Rev. **115**, 98 (1959); W. R. Gibbs and W. Tobocman, *ibid.* **124**, 1496 (1961); W. R. Gibbs and W. Tobocman, *ibid.* **126**, 1076 (1962).

[2] R. H. Bassel, R. M. Drisko, and G. R. Satchler, AEC Report ORNL-3240, 1962 (unpublished).

[3] B. Buck and P. E. Hodgson, Phil. Mag. **6**, 1371 (1961).

[4] W. R. Smith and E. V. Ivash, Phys. Rev. **131**, 304 (1963).

[5] A. Dar, A. de-Shalit, and A. S. Reiner, Phys. Rev. **131**, 1732 (1963).

[6] N. Austern, R. M. Drisko, E. C. Halbert, and G. R. Satchler, Phys. Rev. **133**, B3 (1964).

[7] A preliminary report of this work is contained in the Proceedings of the Conference on Nuclear Spectroscopy with Direct Reactions, Vol. I, Argonne National Laboratory, ANL-6848 (unpublished).

[8] J. R. Erskine, W. W. Buechner, and H. A. Enge, Phys. Rev. **128**, 720 (1962).

tion for a proton, $\psi_d^{(+)}$ is the exact scattering function for incident deuteron waves, V_{np} is the neutron-proton potential, u is the internal wave function of the target, and v is the internal wave function of the residual nucleus. The $G_n=\int d\xi\, u^* v$ is the "wave function of the captured neutron." The shape of this wave function is taken to be a harmonic-oscillator function within the target and a Hankel function times a spherical harmonic without. To represent $\psi_d^{(+)}$ we take an eigenfunction of the Hamiltonian $H_D=H_R+H_r+V_s$, where

$$H_R=T_R+\frac{Ze^2}{R}+V_{\rm opt}(R)\,, \tag{4}$$

$$H_r=T_r+V_{np}(r)\,, \tag{5}$$

$$V_{\rm opt}(R)=(V+iW)\Big/\left[1+\exp\left(\frac{R-R_0}{A}\right)\right]$$
$$=\text{Saxon-well optical potential}, \tag{6}$$

$$V_s=V_{\rm Cp}+V_{\rm op}=\text{polarizing potential}, \tag{7}$$

$$V_{\rm Cp}=Ze^2\left(\frac{1}{|\mathbf{R}+\tfrac{1}{2}\mathbf{r}|}-\frac{1}{R}\right)=\text{Coulomb polarizing potential} \tag{8}$$

$$=Ze^2\left(\frac{-1}{R}+\sum_\lambda\frac{(-\rho_<)^\lambda}{\rho_<^{\lambda+1}}P_\lambda(\hat r\cdot\hat R)\right), \tag{9}$$

$$\rho_<=\min(r/2,R)\,, \tag{10}$$

$$\rho_<=\max(r/2,R)\,, \tag{11}$$

$P_\lambda(\hat r\cdot\hat R)=$Legendre polynomial of cosine of angle between unit vectors $\hat r$ and $\hat R$,

$$V_{\rm op}=V_{\rm opt}(|\mathbf{R}+\tfrac{1}{2}\mathbf{r}|)-V_{\rm opt}(R)=\text{optical polarizing potential}. \tag{12}$$

We neglect $V_{\rm op}$ but allow $V_{\rm opt}(R)$, already present in the Tobocman program, to remain.

The eigenfunction $\psi_d^{(+)}(\mathbf{R},\mathbf{r})$ is handled by the adiabatic approximation. Thus

$$\psi_d^{(+)}(\mathbf{R},\mathbf{r})=F_{ds}^{(+)}(\mathbf{R})\phi_d(\mathbf{r},\mathbf{R})\,, \tag{13}$$

where

$$(H_r+V_{\rm Cp})\phi_d=[\epsilon_0+\epsilon_2(R)]\phi_d\,, \tag{14}$$

$$[H_R+\epsilon_2(R)]F_{ds}=E_dF_{ds}\,, \tag{15}$$

E_d being the center-of-mass kinetic energy of the incident deuteron, ϵ_0 being the negative of the deuteron binding energy, and $\epsilon_2(R)$ the perturbation to ϵ_0 due to Coulomb polarization.

To calculate ϕ_d and $\epsilon_2(R)$ we use perturbation theory, assuming the excited states of the deuteron to be free-particle states. Then

$$\phi_d(\mathbf{r},\mathbf{R})=\phi_0(\mathbf{r})+\phi_1(\mathbf{r},\mathbf{R})+\phi_2(\mathbf{r},\mathbf{R})\,, \tag{16}$$

where ϕ_0 is the Hulthén wave function and ϕ_1 and ϕ_2 are the first- and second-order perturbations due to $V_{\rm Cp}$ which is approximated by its dipole component cutoff by a step function for $r>2R$. The function $\epsilon_2(R)$ is approximated by the second-order energy perturbation due to the dipole. In the latter case, the branch of the dipole expression valid for $r<2R$ is used for all values of r; but a cutoff is imposed for $R<R_0$, where R_0 is the nuclear radius. For Coulomb stripping these approximations are good since the significant region of integration of the T matrix is that for $r\ll 2R$ and $R>R_0$. The explicit expressions used for calculations are as follows:

$$\phi_1(r,R)=\int\frac{d^3k}{\epsilon_0-\epsilon_k}\phi_k^{(r)}\langle\phi_k|V_{c1}|\phi_0\rangle\,, \tag{17}$$

$$\phi_2(r,R)=\int\frac{d^3k}{\epsilon_0-\epsilon_k}\phi_k^{(r)}\int_0\frac{d^3q}{\epsilon_0-\epsilon_q}\langle\phi_k|V_{c1}|\phi_q\rangle\times\langle\phi_q|V_{c2}|\phi_0\rangle\,, \tag{18}$$

$$\epsilon_2(R)=S(R-R_0)\int\frac{d^3k}{\epsilon_0-\epsilon_k}|\langle\phi_0|U_{c1}|\phi_k\rangle|^2\,, \tag{19}$$

where

$$U_{c1}(r,R)=-\frac{Ze^2r}{2R^2}(\hat r\cdot\hat R)\,, \tag{20}$$

$$V_{c1}(r,R)=U_{c1}(r,R)S(2R-r)\,, \tag{21}$$

$$S(a-b)=1 \quad \text{if} \quad a>b$$
$$=0 \quad \text{if} \quad a\le b\,, \tag{22}$$

$$\phi_k(\mathbf{r})=e^{i\mathbf{k}\cdot\mathbf{r}}/(2\pi)^{3/2}. \tag{23}$$

The function $F_{ds}(R)$ was calculated numerically by entering the subroutine of the program which calculates $F_d(R)$, the eigenfunction of H_R, and inserting the additional potential $\epsilon_2(R)$. The wave functions on the left-hand side of the matrix element were calculated to second order by Taylor series in $\mathbf{r}$ about $\mathbf{R}$. For V_{np} we assume the Hulthén potential.

Calculating to second order, we can now express the T matrix as the sum of the following nonzero elements[9,10]:

$$T_1=\langle F_p^{(-)}(\mathbf{R})G_n(\mathbf{R})\,|\,V_{np}(r)\,|\,F_{ds}^{(+)}(\mathbf{R})\phi_0(r)\rangle\,, \tag{24}$$

$$T_2=\langle[\tfrac{1}{2}\mathbf{r}\cdot\boldsymbol{\nabla}_p F_p^{(-)}(\mathbf{R})]G_n(\mathbf{R})\,|\,V_{np}(r)\,|\times F_{ds}^{(+)}(\mathbf{R})\phi_1(\mathbf{r},\mathbf{R})\rangle\,, \tag{25}$$

$$T_3=-\langle F_p^{(-)}(\mathbf{R})[\tfrac{1}{2}\mathbf{r}\cdot\boldsymbol{\nabla}_n]G_n(\mathbf{R})\,|\,V_{np}(r)\,|\times F_{ds}^{(+)}(\mathbf{R})\phi_1(\mathbf{r},\mathbf{R})\rangle\,, \tag{26}$$

$$T_4=\tfrac{1}{2}\langle\tfrac{1}{2}\mathbf{r}\cdot(\boldsymbol{\nabla}_p-\boldsymbol{\nabla}_n)]^2F_p^{(-)}(\mathbf{R})G_n(\mathbf{R})\,|\,V_{np}(r)\,|\times F_{ds}^{(+)}(\mathbf{R})\phi_0(\mathbf{r},\mathbf{R})\rangle\,, \tag{27}$$

$$T_5=\langle F_p^{(-)}(\mathbf{R})G_n(\mathbf{R})\,|\,V_{np}(r)\,|\,F_{ds}^{(+)}(\mathbf{R})\phi_{20}(\mathbf{r},\mathbf{R})\rangle\,, \tag{28}$$

[9] Other apparent elements vanish because of angular-momentum or parity considerations. We have not included the terms arising from the polarization of the target, namely virtual Coulomb excitation, because these are expected to be small (Ref. 5).

[10] For simplicity we assume the target has infinite mass.

where ∇_p acts only on $F_p^{(-)}$, ∇_n acts only on G_n, and ϕ_{20} is the $l=0$ component of ϕ_2. Except for the inclusion of ϵ_2 in computing F_{ds}, T_1 would be the matrix element normally computed by a zero-range program. The terms T_2, T_3, and T_5 represent primarily the contribution due to the corrections in the internal deuteron wave function. There is also a higher order contribution due to the use of F_{ds} in place of F_d. The term T_4, apart from the higher order effect due to the use of F_{ds}, may be regarded as characterizing those finite-range effects remaining when the stretch of the deuteron is neglected.

We now show, using a standard method, that T_4 is very closely a multiple of T_1 and thus has virtually no effect on the shape of the angular distribution

$$T_4=\frac{1}{8}\int\int d^3R d^3r\, F_{ds}^{(+)}(\mathbf{R})[r\cdot(\nabla_p-\nabla_n)^2] \times F_p^{(-)*}(\mathbf{R})G_n(\mathbf{R})V_{np}(r)\phi_0(r) \quad (29)$$

$$=\frac{1}{24}\int d^3R\, F_{ds}^{(+)}(\mathbf{R})(\nabla_p-\nabla_n)^2F_p^{(-)*}(\mathbf{R})G_n(\mathbf{R}) \times\int d^3r\, r^2V_{np}\phi_0^{(+)}. \quad (30)$$

By partial integration and use of the Schrödinger equation, we have the operator equation

$$\begin{aligned}&(\nabla_p-\nabla_n)^2\\&=2(\nabla_p^2+\nabla_n^2)-\nabla_d^2\\&=(-4M/h^2)(T_p+T_n-T_d)\\&=(-4M/h^2)[(E_p+E_n-E_d)-(V_p+V_n-V_d)]\end{aligned} \quad (31)$$

in obvious notation.

In the Coulomb stripping region we can neglect the nuclear portions of the potentials and using conservation of energy we are left with

$$(\nabla_p-\nabla_n)^2=(-4M/h^2)[\epsilon_0+\epsilon_2(R)] \quad (32)$$

$$\approx(-4M/h^2)\epsilon_0=4\alpha^2, \quad (33)$$

where α is the wave number of the deuteron. Thus

$$T_4=\frac{\alpha^2}{6}\int d^3R\, F_p^{(-)*}(\mathbf{R})G_n(\mathbf{R})F_{ds}^{(+)}(\mathbf{R}) \times\int d^3r\, r^2V_{np}\phi_0=0.02T_1 \quad (34)$$

for the Hulthén wave function defined as

$$\phi_0=\left[\frac{\alpha\beta(\beta+\alpha)}{2\pi(\beta-\alpha)^2}\right]^{1/2}\left[\frac{1}{r}(e^{-\alpha r}-e^{-\beta r})\right].$$

RESULTS

With the aid of the modified Gibbs-Tobocman program, a series of runs was conducted for a Bi target over a wide range of incident energy E_d, Q values, and

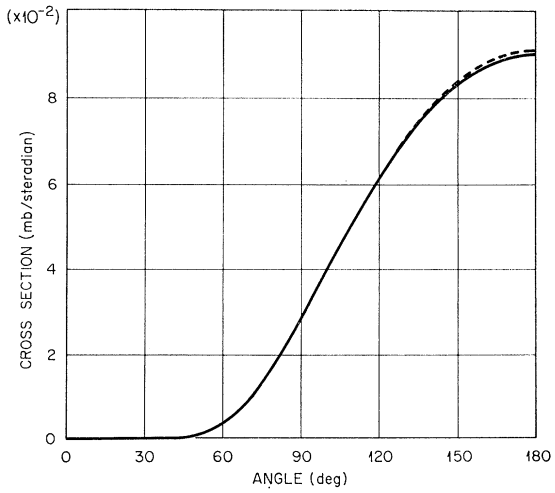

FIG. 1. Comparison of zero-range and modified differential cross sections for a Bi target with $l_n=0$, $E_d=8$ MeV, and $Q=-1.8$ MeV.

captured neutron angular momenta (l). This parameter space was explored freely and not restricted to values corresponding to actual physical levels. Although emphasis was on the Coulomb stripping region, some runs were conducted well outside this region. The region widely explored is delimited as follows:

Parameter	Maximum value	Minimum value
l	2	0
E_d	14 MeV	6 MeV
Q	8 MeV	−1.8 MeV

Some runs were made for $l=4$ and for a few cases E_d ranged as high as 18 MeV and Q as high as 20 MeV.

The Gibbs-Tobocman program employs a Saxon well [Eq. (6)] for the deuteron and proton optical potential.

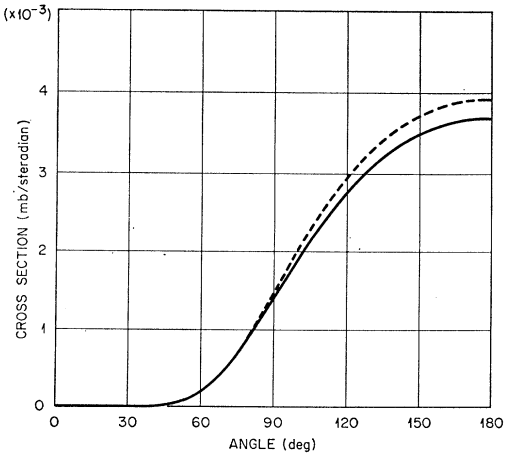

FIG. 2. Comparison of zero-range and modified differential cross sections for a Bi target with $l_n=0$, $E_d=8$ MeV and $Q=-0.203$ MeV.

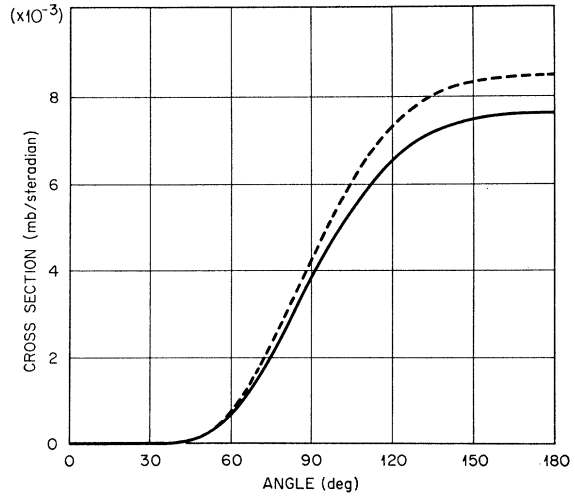

FIG. 3. Comparison of zero-range and modified differential cross sections for a Bi target with $l_n=0$, $E_d=8$ MeV, and $Q=+2$ MeV.

The following parameters were used for all runs:

$$V_d=-50 \text{ MeV}, \quad V_p=-60 \text{ MeV},$$
$$W_d=-15 \text{ MeV}, \quad W_p=-10 \text{ MeV},$$
$$A_d=0.7 \text{ F}, \quad A_p=0.4 \text{ F},$$
$$R_d=8.6 \text{ F}, \quad R_p=7.12 \text{ F}.$$

These are not the latest parameters for optical-model fits, but they serve for our purpose.

The neutron Hankel function was taken outside of the neutron radius $R_n=7.0$ F.

The above optical parameters lead to Coulomb barrier heights of about 10 MeV for the deuteron and 13 MeV for the proton. The Coulomb-stripping region is regarded in this paper as that region in which $E_d \leq 10$ MeV and $E_d+Q \leq 13$ MeV.

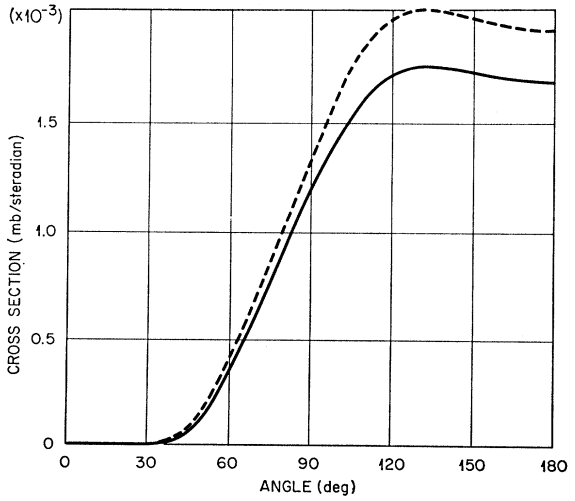

FIG. 4. Comparison of zero-range and modified differential cross sections for a Bi target with $l_n=0$, $E_d=8$ MeV, and $Q=+4$ MeV.

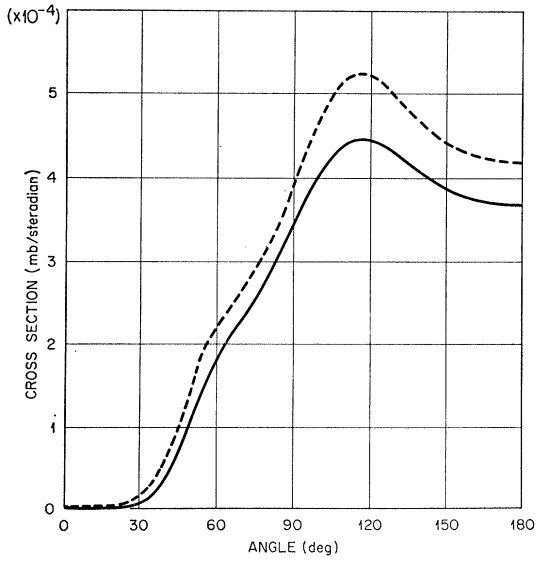

FIG. 5. Comparison of zero-range and modified differential cross sections for a Bi target with $l_n=0$, $E_d=8$ MeV, and $Q=+6$ MeV.

For each computer run the modified and unmodified differential cross sections were plotted on the cathode-ray tube attached to the IBM 7090 and photographed. A sampling of these curves is displayed in Figs. 1–11. Figures 1 through 8 represent a sequence of cases for an $l=0$ captured neutron holding the incident energy E_d fixed at 8 MeV and allowing Q to vary from -1.8 MeV to an unphysically large 20 MeV. We note that the shape of the distribution is not significantly altered and the peak magnitude is only modestly affected until we are well outside the Coulomb-stripping range and at unphysically large Q values. Figures 9 and 10 corre-

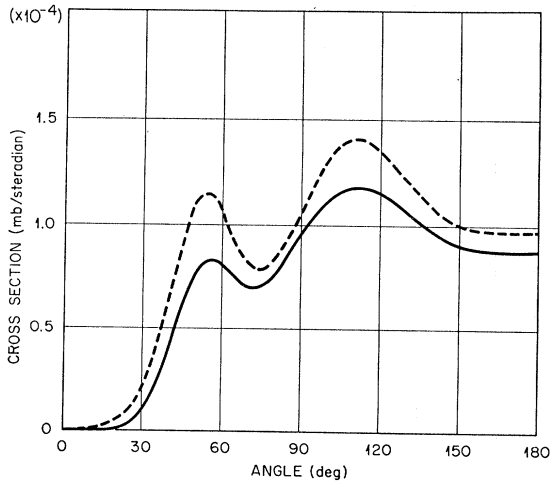

FIG. 6. Comparison of zero-range and modified differential cross sections for a Bi target with $l_n=0$, $E_d=8$ MeV, and $Q=+8$ MeV.

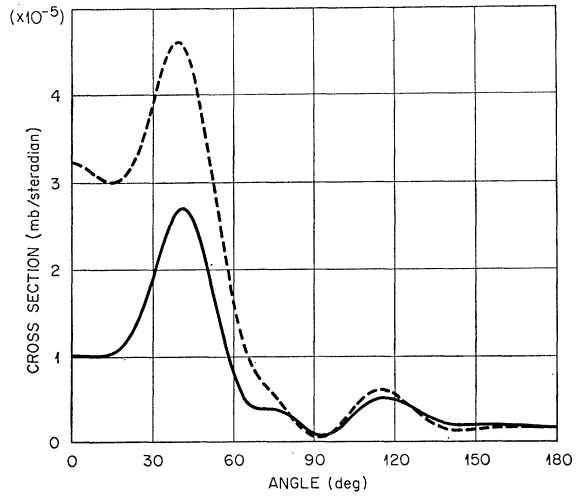

FIG. 7. Comparison of zero-range and modified differential cross sections for a Bi target with $l_n=0$, $E_d=8$ MeV, and $Q=+14$ MeV.

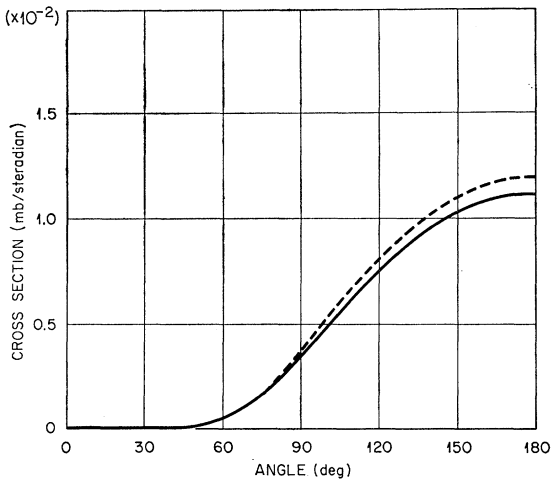

FIG. 9. Comparison of zero-range and modified differential cross sections for a Bi target with $l_n=2$, $E_d=8$ MeV, and $Q=-0.203$ MeV.

spond to Figs. 2 and 4 except that we have an $l=2$ neutron. Note that the alteration is still modest. Figure 11 represents a case of high incident energy and low Q. Again the change is slight.

The results of all runs are summarized in Table I. We observe that the % deviations for Coulomb stripping are moderate and range up to 16%. Except for a few cases of high E_d and low Q the cross section is increased. The deviation seems to be independent of the l value of the captured neutron.

A number of additional runs were made to determine the relative effects of the modifications separately. Figure 12 portrays a breakdown of the contributions from the various matrix elements to the peak differential cross section of an 8-MeV deuteron over a range of Q values with $l=0$, while Figs. 13 and 14 portray the same breakdown as a function of incident deuteron energy for two fixed Q values. The curve labeled "all effects" depicts the relative deviation when all modifications were used. The curve labeled "external polarization effect" is derived from the use of matrix element T_1 alone and represents the deviation generated by use of the modified center-of-mass deuteron wave function F_{ds}. The curve labeled "finite-range effect" is the flat contribution from T_4 as previously discussed. The curve labeled "internal polarization effect" represents the deviation resulting from adding T_2, T_3, and T_5 to the unmodified matrix element. These three elements are the only ones incorporating a correction to the internal

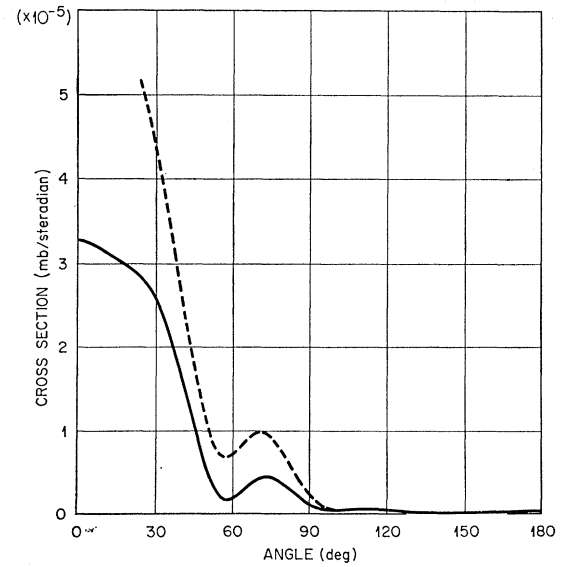

FIG. 8. Comparison of zero-range and modified differential cross sections for a Bi target with $l_n=0$, $E_d=8$ MeV, and $Q=+20$ MeV.

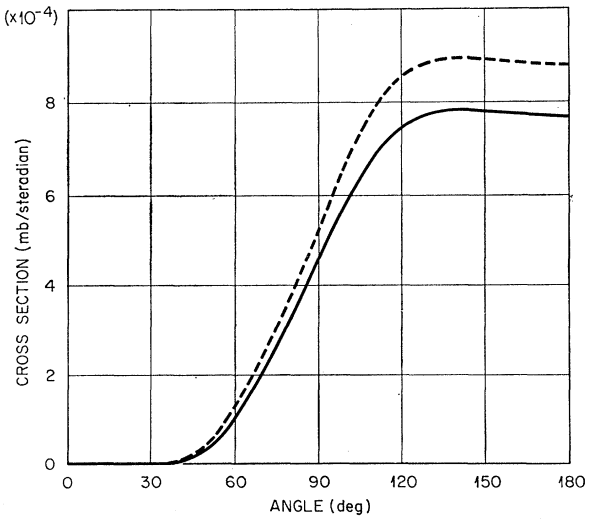

FIG. 10. Comparison of zero-range and modified differential cross sections for a Bi target with $l_n=2$, $E_d=8$ MeV, and $Q=+4$ MeV.

TABLE I. Percent deviation of peak of modified differential cross section from the peak of the Gibbs-Tobocman cross section. The region printed in italics in each section of the table is the Coulomb-stripping region (see text).

		Q (MeV)							
l	E_d (MeV)	−1.8	−0.203	+2.0	+4.0	+6.0	+8.0	+14.0	+20.0
0	6		*6.4*	*10.5*	*13.9*	*16.2*	17.1		
	8	*1.1*	*6.7*	*11.4*	*14.3*	16.9	19.2	69.8	101.8
	10	*−4.8*	*2.0*	*7.2*	9.8	23.0	34.9		
	12	−6.2	−1.1	2.6	10.5	14.5	22.8		
	14	−6.2	−3.6	3.7	9.3	14.1	18.2		
	16		−3.7		9.2				
	18		0.5						
2	6		*6.6*		*13.8*	*16.0*	17.4		
	8	*2.3*	*7.2*	*11.7*	*14.3*	17.0	19.2		
	10		*2.3*	*7.2*	10.3				
	12	−2.0	0.8		11.3		31.0		
	14								
4	6		*7.1*						
	8		*8.2*		*14.8*		18.6		
	10				9.6				
	12		2.7		5.5[a]				

[a] The angular distribution is twin peaked. The deviation for the other peak is 14.1%.

deuteron wave function. We see that their contribution is on the order of 1% or less and that major contributions come from T_4 and the use of the modified scattering wave function for the deuteron. These observations are borne out by other runs, the results of which are summarized in Table II. "σ_{1S}" corresponds to the "ex-

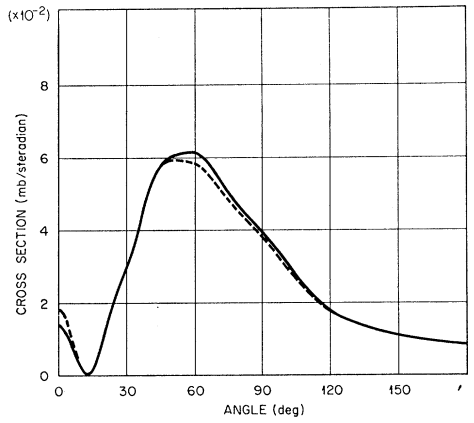

FIG. 11. Comparison of zero-range and modified differential cross sections for a Bi target with $l_n=0$, $E_d=16$ MeV, and $Q=-0.203$ MeV.

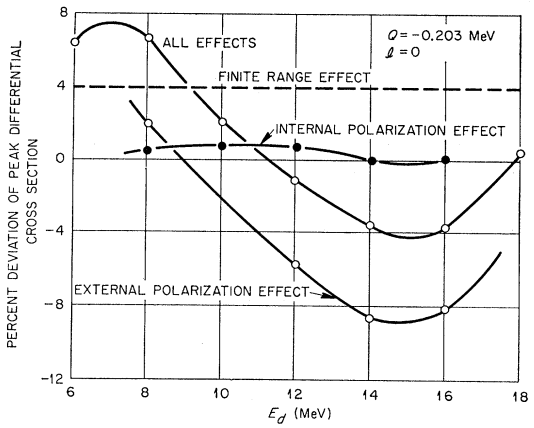

FIG. 13. Comparison of polarization and finite-range effects as a function of incident deuteron energy for $Q=-0.203$ MeV and bound-state $l=0$. Target is Bi.

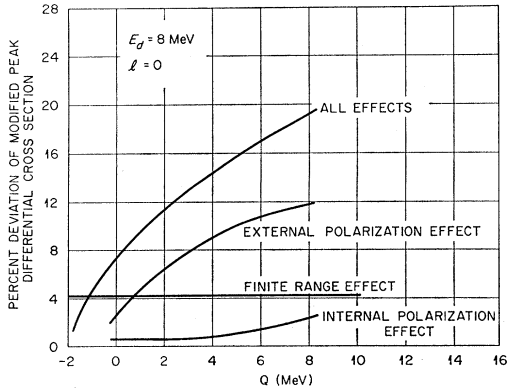

FIG. 12. Relative influence of the three classes of modifications upon the peak zero-range differential cross section as a function of Q with $l_n=0$ and $E_d=8$ MeV.

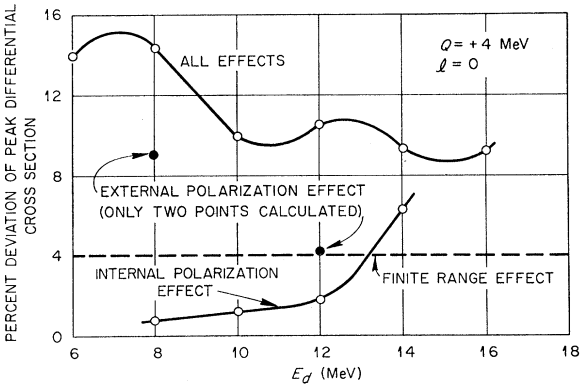

FIG. 14. Comparison of polarization and finite-range effects as a function of incident deuteron energy for $Q=+4$ MeV and bound state $l=0$. Target is Bi.

TABLE II. Percent deviation of peak of σ_{1s} and σ_g from peak of Gibbs-Tobocman differential cross section (σ_1).[a]

Deviation of	l	E_d (MeV)	Q (MeV) −0.203	+2.0	+4.0	+6.0	+8.0	+14.0	+20.0
σ_{1s}	0	8	*2.0*	*6.3*	*9.0*	10.8	11.6	20.1	22.1
		10				9.1			
		12	−5.7		1.7				
		14	−8.6						
		16	−8.1						
	2	8				10.5			
σ_g	0	8	*0.51*	*0.58*	*0.74*			34.2	72.7
		10	*0.7*	*1.0*	1.2				
		12	0.7		4.2				
		14	0.0	3.2	6.3				
		16	0.1						
	2	12	0.7		4.9				

[a] The regions printed in italics are in the Coulomb stripping region.

ternal polarization effect" and refers to the peak differential cross section when using T_1 alone. "σ_g" corresponds to the "internal polarization effect" and refers to the peak differential cross section obtained from adding T_2, T_3, and T_5 to the Tobocman matrix element. Note that the σ_{1S} deviation ranges up to 9% and the σ_g deviation up to 1% in the Coulomb-stripping region. For two cases with unphysically large Q values, the deviation of σ_g becomes quite large. These values cannot be taken very seriously since they are well outside the region of validity of our approximations. On a strictly calculational basis, however, these values are not surprising since they correspond to high neutron binding energies. The corresponding rapid decay of the neutron wave functions would greatly accentuate the relative importance of the target region in the calculation of the matrix element and it is in that region that the deuteron internal wave function of our model would be most perturbed.[11]

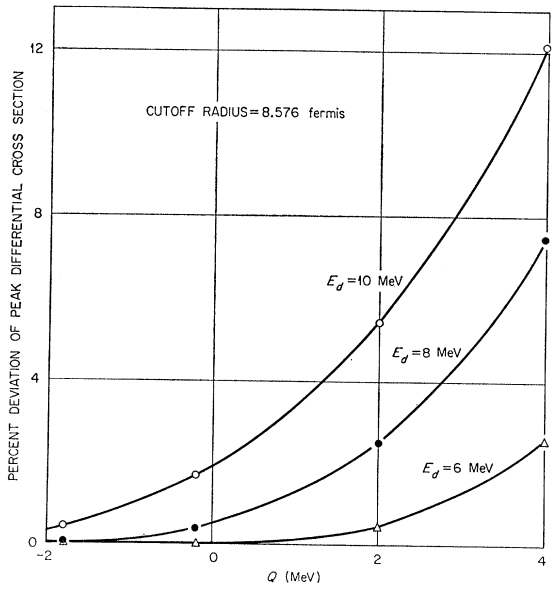

FIG. 15. Effect of imposing a cutoff in zero-range calculation as a function of Q for several incident deuteron energies and a bound state $l=0$. Target is Bi.

These results, namely that the second-order corrections to the zero-range Coulomb-stripping matrix are all small, suggest that our series in **r** is reasonably convergent and that higher order terms would be even smaller. In order to check our fundamental assumption that contributions from the nuclear interior are really small, we have compared our complete calculations with a set for which the internal region was not included. For a cutoff radius of 8.6 F we have plotted in Fig. 15 the percentage of the cross section coming from the interior in our calculations. As expected, this percentage rises with incoming deuteron energy but remains quite small over a range of Q values. It rises with increasing Q value, as discussed above.

Finally we have investigated the effect of the nuclear potentials on the cross sections. Since we already know that the nuclear interior is not important the only effect of these potentials can come through the phase shifts. As has been pointed out to us by Austern and Drisko[12] this effect need not necessarily be small. In Fig. 16 we show the effect of setting the nuclear potentials to zero for $l=0$. We see that the effect can indeed be very large especially for high incident energy and high Q. However, this does not detract from our aim of obtaining a reliable measure of reduced widths, because the phase shifts can be measured from elastic scattering and we need assume nothing about the nuclear interior. The fact[13,14] that recent refinements for the nuclear potential including nonlocal effects actually change the optical wave functions inside by as much as

[11] We are indebted to James Griffin and Leon Heller for discussions on this point.

[12] N. Austern and R. Drisko (private communication).

[13] J. K. Dickens, R. M. Drisko, F. G. Perey, and G. R. Satchler, Phys. Letters **15**, 337 (1965).

[14] F. G. Perey, *Proceedings of International Symposium on Direct Interactions and Nuclear Reaction Mechanisms, Padua, 1962* (Gordon and Breach Science Publishers, Inc., New York, 1963), p. 125.

30% is essentially irrelevant, as long as we stay in the Coulomb-stripping region.

The expression for reduced width as computed by the zero-range program is

$$\gamma = (\hbar^2/2\mu_{IN})R_0 u_l^2(R_0),$$

where γ is the reduced width, $\hbar$ is Planck's constant divided by 2π, μ_{IN} is the reduced mass of the target and captured neutron, R_0 is the nuclear radius, and u_l is the radial portion of the neutron wave function.

Outside the target radius, the true neutron wave function and the one used in the zero-range program differ only by a constant factor. Thus for Coulomb stripping the "true reduced width" may be estimated by

$$\gamma_e = \gamma_c \left[\frac{d\sigma_e}{d\Omega} \Big/ \frac{d\sigma_c}{d\Omega} \right],$$

where the subscript c refers to numbers computed by the program and e to experimental results. The effect of the program modifications on γ_e will thus be inverse to the effect on $d\sigma_e/d\Omega$ (since γ_c is not changed). Thus, for example, for 8-MeV deuterons, $\gamma_e \approx 0.16$ MeV for the 2.57-MeV level of ^{210}Bi as obtained from the zero-range program and Erskine's[8] data. The modified program reduces this about 6%.

CONCLUSIONS

One concludes that in the stripping region for a Bi target the finite-range and polarization effects usually increase the differential cross section and reduce the estimate of the reduced width by a variable amount of not more than about 16%, and usually considerably less (Figs. 12–14).

Within the Coulomb-stripping region the cross-section deviations are largely generated by the external-polarization and finite-range modifications. The internal polarization modification generates only on the order of 1% or less. The finite-range modification by itself introduces a 4% increase in the cross section at all angles. The relative change in peak differential cross section from all modifications was essentially insensitive to the l value of the captured neutron. These conclusions are numerically based on employment of a Hulthén potential and wave function. Other deuteron potentials and wave functions will be tried in future work.

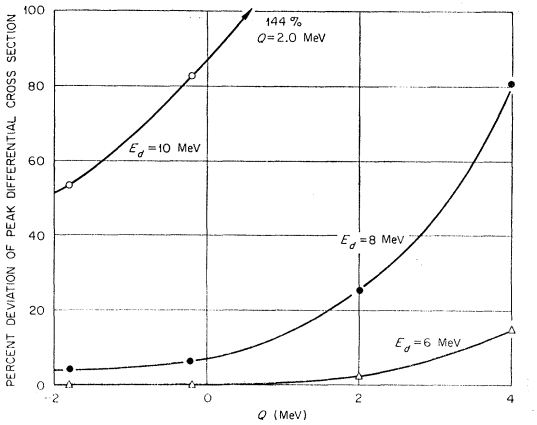

FIG. 16. Effect of setting nuclear potentials to zero in zero-range calculation as a function of Q for several incident deuteron energies and a bound state $l=0$. Target is Bi.

An experimental test of these conclusions would be to do Coulomb stripping as a function of energy. The reduced widths should then be independent of energy to the accuracy of the above approximations.

ACKNOWLEDGMENTS

The authors are indebted to Professor R. H. Lemmer for many fruitful discussions regarding this work. We also wish to acknowledge the advice and service of the MIT Computation Center.